CrossMark

Experimentally-determined carbon isotope fractionation in and between methane-bearing melt and fluid to upper mantle temperatures and pressures

Bjorn Mysen

Geophysical Laboratory, Carnegie Instn., Washington, USA

ARTICLE INFO

ABSTRACT

The behavior of melts and fluids is at the core of understanding formation and evolution of the Earth. To advance our understanding of their role, high-pressure-/temperature experiments were employed to determine melt and fluid structure together with carbon isotope partitioning within and between $(CH_4 + H_2O + H_2)$-saturated aluminosilicate melts and $(CH_4 + H_2O + H_2)$-fluids. The samples were characterized with vibrational spectroscopy while at temperatures and pressures from 475° to 850°C and 92 to 1158 MPa, respectively.

The solution equilibrium is $2CH_4 + Q^n = 2CH_3^- + H_2O + Q^{n+1}$ where the superscript, n, in the Q^n-notation describes silicate species where n denotes the number of bridging oxygen. The solution equilibrium affects the carbon isotope fractionation factor between melt and fluid, $\alpha^{melt/fluid}$. Moreover, it is significantly temperature-dependent. The $\alpha^{melt/fluid} < 1$ with temperatures less than about 1050°C, and is greater than 1 at higher temperature.

Methane-bearing melts can exist in the upper mantle at $f_{O_2} \leq f_{O_2}(MW)$ (Mysen et al., 2011). Reduced (C–H)-species in present-day upper mantle magma, therefore, are likely. During melting and crystallization in this environment, the $\delta^{13}C$ of melts increases with temperature at a rate of $\sim 0.6\%/°C$. From the simple-system data presented here, at $T \leq 1050°C$, melt in equilibrium with a peridotite-$(CH_4 + H_2O + H_2)$-bearing mantle source will be isotopically lighter than fluid. At higher temperatures, melts will be isotopically heavier. Degassing at $T \leq 1050°C$ will shift $\delta^{13}C$ of degassed magma to more positive values, whereas degassing at $T \geq 1050°C$, will reduce the $\delta^{13}C$ of the degassed magma.

1. Introduction

The budget and recycling of volatile components in the Earth's interior govern the formation and evolution of the solid Earth, its oceans, and atmosphere (e.g., Kasting et al., 1993; Tolstikhin and Marty, 1998). Tracing the role of volatile components often relies on understanding the behavior of isotopes such as those of hydrogen, carbon, nitrogen, and sulfur (Dixon et al., 1997; Van Soest et al., 1998). As these elements can exist in different oxidation states in the range of redox conditions of the Earth's interior (e.g., Saxena and Fei, 1987; Luth et al., 1990), their redox state can affect their isotope fractionation behavior (Ohmoto, 1972; Richet et al., 1977). An understanding of stable isotope behavior during magmatic processes, therefore, requires characterization of the redox conditions as well as temperature and pressure.

In the C–O–H system of volatiles, methane (CH_4) is a principal carbon-bearing species under redox conditions such as those existing during separation of iron-rich metal from an extensively melted Earth to form its core (below that described by the iron–wustite oxygen buffer; Ohmoto and Kerrick, 1977; O'Neill, 1991; Righter and Drake, 1999). It has been reported recently, however, that even under less reducing conditions such as those of the magnetite–wustite (MW) oxygen buffer, CH_4 is the dominant C-bearing species in silicate melts (Mysen et al., 2011). Such redox conditions are near those typical of the present day upper mantle (e.g., Bryndzia and Wood, 1990; McCammon, 2005).

A few experimental data exist for quenched silicate melts equilibrated with $(CH_4 + H_2O + H_2)$-fluid at magmatic temperatures and upper mantle pressures. Those data indicate that silicate melt structure can have profound effect on $^{13}C/^{12}C$ fractionation between melt and fluid (Mysen et al., 2009). This conclusion relies, however, on the assumption that temperature-quenching of high-temperature melt to form a glass for analysis ambient con-

*E-mail address:* bmysen@carnegiescience.edu.

ditions does not change its composition and structure. Silicate melt structure is, however, temperature-dependent (see, for example, review of such structural information by Mysen and Richet, 2005). Melt composition also can change because minerals sometimes crystallize from melt during temperature-quenching thus altering their composition. This can be a particular problem when quenching volatile-rich melt from high temperature at high pressure (e.g., Mysen et al., 1974; Baker and Stolper, 1994). Moreover, quench precipitation of oxide materials from fluids equilibrated at high temperatures and pressures is common (Mysen and Acton, 1999; Kessel et al., 2004). This material must be separated from quenched melts before analysis. Such separation is often challenging. Incomplete separation of quench precipitates from quenched melts will affect melt analytical data.

In order to avoid the complications that often arise from temperature-quenching of high-temperature/-pressure experimentally-equilibrated samples, structural and isotopic characterization of coexisting fluids and melts while at the temperatures and pressures of interest is desirable. The data in the present report were obtained in this manner. Carbon speciation and carbon isotope ratio of melts and fluids were determined by vibrational spectroscopic methods. These measurements were carried out while the samples, contained in hydrothermal diamond anvil cells, were at the temperatures, pressures, and redox conditions of interest. A compositionally simple ternary alkali aluminosilicate melt was used in the study in order to facilitate interpretation of vibrational spectra. It is emphasized, therefore, that the reported data serve to illustrate principles that describe carbon isotope fractionation in and between coexisting melt and fluid to upper mantle temperatures and pressures. However, given the chemical simplicity compared with natural magmatic melts, quantitative application of the experimental results to natural magmatic processes should be carried out with caution.

2. Experimental methods

High-temperature/-pressure experiments were carried out with externally-heated hydrothermal diamond cells (HDAC) of the type described by Bassett et al. (1996). The upper and lower diamonds were surrounded by Mo-wound heaters. Aluminosilicate glass, C–O–H fluid, a reducing agent (Ti metal), and a pressure sensor (synthetic ^{13}C diamond) starting materials were contained in a 500 μm-diameter central hole of 125 μm thick, polished Ir gaskets. Before an experimental measurement series, the gaskets were work-hardened to the highest temperatures and pressures to minimize sample volume changes during experiments.

The silicate portion of the starting material consisted of several ≤100 μm chips of a Na aluminosilicate glass [$(Na_2Si_4O_9)_{90} \cdot (Na_2(NaAl)_4O_9)_{10}$], also used in previously for high-temperature/ pressure examination of water solution mechanisms in silicate melts (Mysen, 2007, 2015). The carbon component of the fluid was added as $Ag_2C_2O_4$ followed by double-distilled, dionized and filtered H_2O. The starting $Ag_2C_2O_4$ was a 50:50 mixture of ^{13}C and ^{12}C. It was synthesized from an aqueous solution of a 50:50 mixture of $H_2^{13}C_2O_4$ and $H_2^{12}C_2O_4$ by reaction with $AgNO_3$ in aqueous solution. The $Ag_2C_2O_4$ breaks down to CO_2 and metallic Ag near 150 °C. Powdered Ti metal was added to serve as reducing agent to convert $CO_2 + H_2O$ to $CH_4 + H_2$ (Foustoukos and Mysen, 2012) via the reaction,

$$CO_2 + 4H_2O + 3Ti = CH_4 + 2H_2 + 3TiO_2. \quad (1)$$
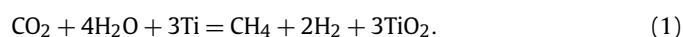
The oxygen fugacity (f_{O_2}) of the $Ti + O_2 = TiO_2$ reaction at the temperatures of the present experiments is about 15 orders of magnitude lower than that required for CH_4 to dominate the C–O–H species (Robie et al., 1978; Ohmoto and Kerrick, 1977). Metallic

Ti in the presence of H_2O is, therefore, a very efficient means by which to produce CH_4 from $CO_2 + H_2O + Ti$.

Temperature was measured with two K-type thermocouples in contact with the upper and lower diamonds, respectively, and located less than 1 mm from the sample area. Temperature precision was ±1 °C and uncertainty ±3 °C from calibration against the NaCl melting temperature (800.5 °C) at ambient pressure. Pressure, generated with changes in temperature in a near-fixed volume sample chamber, was monitored with the 1st-order Raman shift of synthetic ^{13}C diamond from 10–20 μm diamond pieces mixed in with the sample (Schiferl et al., 1997). With this arrangement, precision was ±40 MPa, whereas uncertainty is ±110 MPa (Mysen and Yamashita, 2010).

Aluminosilicate-saturated ($CH_4 + H_2O + H_2$)-fluid and coexisting ($CH_4 + H_2O + H_2$)-saturated aluminosilicate melts were monitored optically with optical microscopy at 500X magnification and characterized with Raman spectroscopy while in the HDAC at the temperature and pressure conditions of interest. Melt and fluid structure and the carbon isotope ratios were determined with a JASCO model NSR3100 confocal micro-Raman system equipped with an Olympus microscope, a single monochromator, holographic notch filter, and holographic gratings. A 2.5 cm working distance, Mito-toyo, 50X/0.42 N.A. objective lens was attached to the Olympus microscope for the optical observations and backscatter Raman measurements. Spectra were recorded with an Andor Model DV401-F1 1024 × 128 pixel, Peltier-cooled CCD operating at ∼ −70 °C. The samples were excited with 30–35 mW power of the 490.2 nm line of a solid state Coherent™ laser. The beam diameter at the sample was 2–3 μm. Confocal optics limits to ∼30 μm the depth of excitation of optically clear samples (Mysen, 2015). Groove density of the holographic gratings for sample measurements was 1200 grooves/mm, which resulted in ±3 cm^{-1} frequency uncertainty. To determine the Raman shift of the ^{13}C diamond for pressure determination, 2400 grooves/mm were used (±1 cm^{-1} frequency uncertainty). The frequency uncertainty of these latter measurements was reduced to ±0.1 cm^{-1} by using Ne emission lines as internal frequency standard.

Raman spectra of each melt + fluid sample were recorded at a series of pressure and temperature conditions. The temperature separation between each condition was 50–75 °C. The measurements were carried out following about 60 min dwell time at each temperature, which is sufficient to reach equilibrium in experiments under conditions such as those employed here (Horita, 1988). That conclusion also is consistent with HFSE solubility measurements in aqueous fluid equilibrating with crystalline oxides (Wilke et al., 2012).

3. Results

Fluid and melt coexisted over the entire temperature- and pressure range of the experiments. A straight-line fit through the pressure/temperature data points (Fig. 1) was used to obtain an approximate pressure corresponding to a temperature and used in the figures where temperature is an independent variable as a reminder that unless otherwise stated, there is a temperature-dependent pressure for each temperature.

3.1. Raman spectra

Fluid and melt spectra in the 300–1200 cm^{-1} frequency range are different (Fig. 2). Those of fluids have a sharp peak, marked R$_1$, near 600 cm^{-1}, one or two peaks between 00 and 850 cm^{-1} (marked Q and R$_2$), and a sharp peak near 1050 cm^{-1} (R$_3$). The R$_1$, R$_2$, and R$_3$ are the rotational bands from molecular H$_2$ (Taylor and Strauss, 1989). At temperatures and pressures above 700 °C/768 MPa, there is an additional weak peak near 770 cm^{-1}